

EVALUATION OF HYDROGEN EMBRITTLEMENT IN FeAl ASSISTED BY MECHANICAL MILLING

E. García de León^a, O. Téllez-Vázquez^b, C. Patiño-Carachure^c, C. Ángeles-Chávez^d, G. Rosas^{*b}

^a Facultad de Química, Universidad Nacional Autónoma de México, Coyoacán, México D. F., 04510, México.

^b Instituto de Investigaciones Metalúrgicas, UMSNH, Edificio U., Ciudad Universitaria, Morelia, Mich., 58000, México.

^c Facultad de Ingeniería, Universidad Autónoma del Carmen, Campus III, Avenida Central S/N, Esq. con Fracc. Mundo Maya, C.P. 24115, Ciudad del Carmen, Campeche, México.

^d Instituto Mexicano del Petróleo, Eje Central Lázaro Cárdenas No 152, Col. San Bartolo Atepehuacan, México D. F., 07730.

*Corresponding author, e-mail: grtrejo07@yahoo.com.mx

Recibido: Noviembre 2011. Aprobado: Marzo 2013.

Publicado: Mayo 2013.

ABSTRACT

Fe₄₀Al₆₀ (at%) intermetallic alloy composition was obtained by conventional casting methods and subsequently subjected to high-energy mechanical milling under different conditions of humidity. All samples were characterized by X-ray diffraction patterns (XRD) and transmission electron microscopy (TEM) images. Both techniques confirm the formation of bayerite phase and the presence of nano-crystals of FeAl. The presence of bayerite phase is attributed to the hydrogen embrittlement reaction which occurs in the intermetallic material in where hydrogen is released. It is observed that as the milling time increased the bayerite phase is increased and consequently hydrogen is increased too. As observed by TEM results hydrogen contributes in the reduction of crystal size due to the cleavage fracture mechanism. In this way the particles which are surrounded by the bayerite phase reaches nanometric sizes.

Keywords: FeAl, Intermetallic, Hydrogen Embrittlement, Mechanical Milling, Nanoparticles.

EVALUACIÓN DE LA FRAGILIZACIÓN POR HIDRÓGENO EN FeAl ASISTIDA POR MOLIENDA MECÁNICA

RESUMEN

La composición de la aleación intermetálica Fe₄₀Al₆₀ (% at.) se obtuvo por métodos convencionales de colada y posteriormente se sometió a molienda mecánica de alta energía a diferentes condiciones de humedad. Todas las muestras se caracterizaron por medio de patrones de difracción de rayos X e imágenes de microscopía electrónica de transmisión. Ambas técnicas confirman la formación de la fase bayerita y la presencia de nanocristales de FeAl. La presencia de la fase bayerita se atribuye a la reacción de fragilización por hidrógeno que se produce en el material intermetálico en donde el hidrógeno se libera. Se observa que a medida que el tiempo de molienda aumentó la fase bayerita se incrementa y por consiguiente el hidrógeno también aumenta. Como se observó de los resultados de microscopía, el hidrógeno contribuye a la reducción del tamaño del cristal debido al mecanismo de fractura por clivaje. De este modo, las partículas que se encuentran rodeadas por la fase bayerita alcanzan tamaños nanométricos.

Palabras claves: FeAl, Intermetálico, Fragilización por Hidrógeno, Molienda Mecánica, Nanopartículas.

INTRODUCTION

Transition-metal aluminides as Ni, Ti, and Fe, have been extensively investigated due to their excellent structural properties at high temperatures such: low density, good corrosion and oxidation resistance [1-3]. In the particular case of iron aluminide (FeAl), has been a special interest

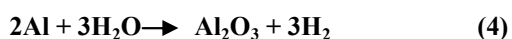
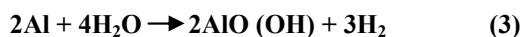
due to their attractive physical and mechanical properties as well as low cost [4-7]. However, it is well known that the FeAl intermetallic compound is susceptible to hydrogen environmental embrittlement (HEE), which limits its applications [3, 7]. The following chemical

reaction is assumed to take place in the HEE process [8,9]:



Where, Al atoms in the intermetallic alloy (FeAl) react with water vapour in the air to produce Al_2O_3 and H_2 . Hydrogen reduces the cohesive force between the atoms and thus promotes brittle fracture by bond rupture [8]. This behavior is increased as the aluminum content in the alloy is increased [8,10]. In some cases, after this phenomenon intermetallic alloy ingots can be converted spontaneously into fine powders [10]. The reduction in the particle size could be of interest in case of particles reaches the nanometer scale. A single research has previously reported about nanoparticles formation through HEE process [11].

On the other hand, in the past it has been demonstrates that the aluminum and its alloys can produce hydrogen from water splitting through the following mechanisms [12-14]:



The products of these reactions are: bayerite, $\text{Al}(\text{OH})_3$ boehmite, $\text{AlO}(\text{OH})$, alumina Al_2O_3 and H_2 , the last one is produced in all reactions. Presumably, when the aluminum in the intermetallic alloy reacts with water to liberate hydrogen, a reduction in crystal size should be occur due to the HEE phenomena. Moreover, the mechanical milling process of a brittle material (intermetallic) should further contribute to the reduction in crystal size. Thus in this study, we present the results obtained of HEE in FeAl intermetallic assisted by mechanical milling to evaluate the reduction in the particle and crystal size, as well as the phases involved after wet-milling process of the pre-alloyed powders.

MATERIALS AND METHODS

FeAl intermetallic alloy was synthesized using an induction furnace (INDUCTOTHERM) of 10 Kg capacity and silicon carbide crucibles. Ingots with a nominal composition of $\text{Fe}_{40}\text{Al}_{60}$ (at %) were prepared. This alloy composition was chosen because it contains a greater amount of aluminum as compared to the stoichiometric ratio (1:1). High aluminum content easily induces embrittlement reaction in FeAl alloy [10]. Has been previously reported that cleavage fracture (HEE) is accentuated when the aluminum in the intermetallic alloy is increased [8,10]. This intermetallic alloy was subsequently subjected to mechanical milling (MM) using a vibratory mill (SPEX 8000). For the experiments, the humidity during ball-milling was 6 ml of deionized H_2O per-gram of alloyed powder used. The milling times were; 1, 2, 4, 6, 8 and 10 h. The ball-to-powder weight ratio used was 10:1. The structural characterization was carried out using a transmission electron microscope (Philips Tecnai F20) and a X-ray diffractometer (XRD Siemens D5000). The average crystal size was estimated from the X-ray broadening of the (110) reflection using Debye-Scherrer equation:

$$t = 0.9\lambda / \beta \cos \theta_\beta \quad (5)$$

Where:

t crystal size

λ $K\alpha$ radiation of Cu (1.5406 Å)

β measured width at half maximum intensity (FWHM)

θ_β angle of diffraction peak

RESULTS AND DISCUSSION

Figure 1 shows the XRD patterns obtained from the $\text{Fe}_{40}\text{Al}_{60}$ as-cast alloy and also from the ingot mechanically milled for different times. The as-cast alloy illustrate in Figure 1a shows the typical cubic B2 structure with lattice parameter; $a = 2.89$ Å corresponding to FeAl intermetallic compound. On the

other hand, the milled samples (Figures 1b-g) show new reflections corresponding to the ceramic compound α -Al(OH)₃ with hexagonal structure and lattice parameters; $a = 5.047 \text{ \AA}$ and $b = 4.73 \text{ \AA}$. This phase is known mineralogically as bayerite (α). It is observed from XRD patterns that as the milling time increased, the relative intensities of the intermetallic phase gradually decreased, while at the same time the intensities of bayerite phase increased.

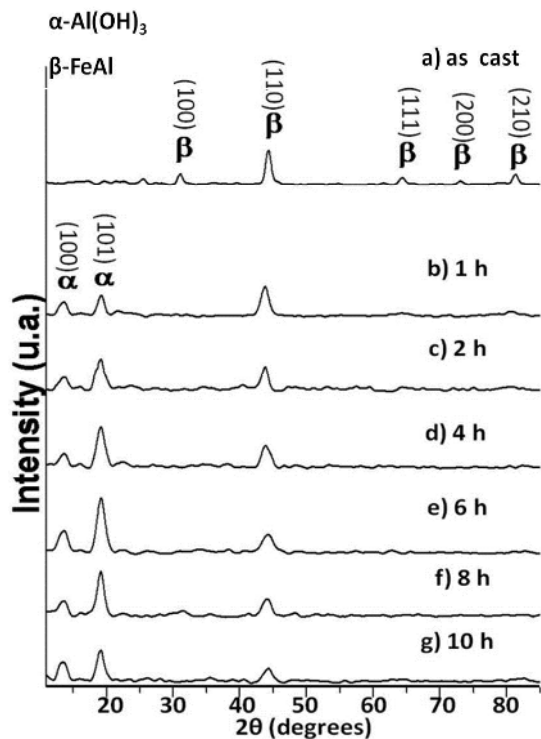


Fig. 1. X-ray diffraction patterns of the samples milled at different times.

Moreover, there is an increase in the width of XRD peaks related to the β -phase, which indicates that the crystal size decreased as the milling time increased. This results indicate that the HEE reaction between the aluminum and water take place in the milling container to the bayerite formation. It is reasonable that, due to the relation between bayerite phase and hydrogen through chemical reaction #2, the hydrogen is also increases as the milling time increased. This also suggests that the mechanism of cleavage fracture of hydrogen should be contributed in the reduction of the crystal size. It is observed that after 10 hours of milling the peaks of the bayerite phase also

are reduced in intensity. This could be due to after 6 hrs of milling, α phase begins to receive mechanical energy from the milling process; this effect is noted by the decrease of the intensity and peak broadening, indicating a decrease in crystal size.

In order to evaluate the crystal size for the FeAl samples milled at different times, the experimental FWHM (full width at half maximum) was measurement from the (110) diffraction peak. These values were used in the Debye-Scherrer equation. Table 1 presents the calculated data of crystal size at different times. The crystal size data are also plotted in Figure 2, which was obtained by ordinary least squares method. This figure describes the evolution of crystal size, which has an exponential decay behavior and its tendency is similar to that reported previously by Suryanarayana [15], but for the samples milled under dry conditions.

Table 1. Crystal size values of FeAl phase as a function of milling time.

Milling time (h)	FWHM (rad)	Crystal size of FeAl phase (nm)
1	0.7794	10
2	0.8660	9
4	0.9266	8
6	1.529	5
8	1.52	5
10	1.518	5

The HAADF-STEM technique gives us an idea of the chemical composition of the material, because the total scattering intensity is proportional to the square of the atomic number, Z^2 . Figure 3 a) and 3 b) correspond to low and higher magnifications of Z-contrast TEM images taken from the sample milled by 6 h and 6ml of humidity. In these images, bright regions correspond to regions (small particles) with higher atomic number, while less bright regions correspond to a phase with low atomic number (bayerite).

The morphology for both types of phases is also different allowing easy phase identification. Furthermore, Figure 3 c) corresponds to the EDS chemical analysis of the sample, where the presence of elements related to both phases is shown; α (Al, O) and β (Fe, Al). Thus, the powders under these experimental conditions consist of nanometer-sized crystals (AlFe) embedded in the ceramic phase, $\text{Al}(\text{OH})_3$. These results are consistent with those obtained from XRD. The small metallic aggregates in both figures have nanometric size ranges between 2–4 nm, which confirm the radical reduction in particle size after the hydrogen embrittlement reaction assisted by ball milling. Due to differences in density, the intermetallic nanocrystals represent a smaller volumetric fraction in comparison to the ceramic phase.

The embrittlement reaction between aluminum in the alloy and water takes place at the interface of solid particles. Therefore, as the reaction proceeds the metal particles are progressively coating with the ceramic material, this indicates that a process of phase separation could be required.

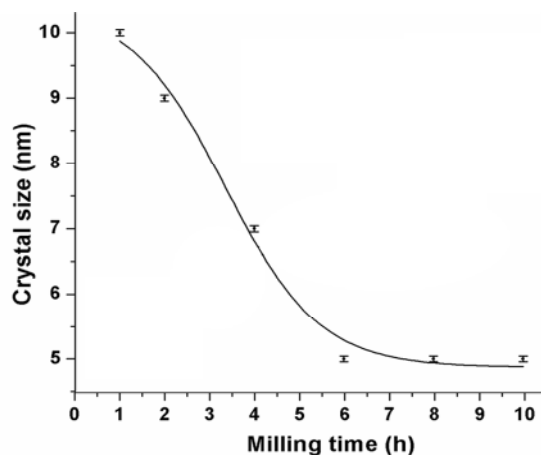


Fig. 2. Evolution of crystal size as a function of the milling time.

Figure 4 shows a dark-field TEM image with its corresponding electron diffraction pattern from the sample milled for 6 h with 6 ml H_2O . The TEM image shows bright spots which are associated with the presence of very small crystallites (<10 nm). The electron

polycrystalline pattern shows the indexed planes: (101), (100) and (001) which corresponds to α phase. Whereas, the rings indexed by (100), (110) planes corresponds to the β phase. These results also confirm that the HEE reaction take place in where the small metallic particles are formed.

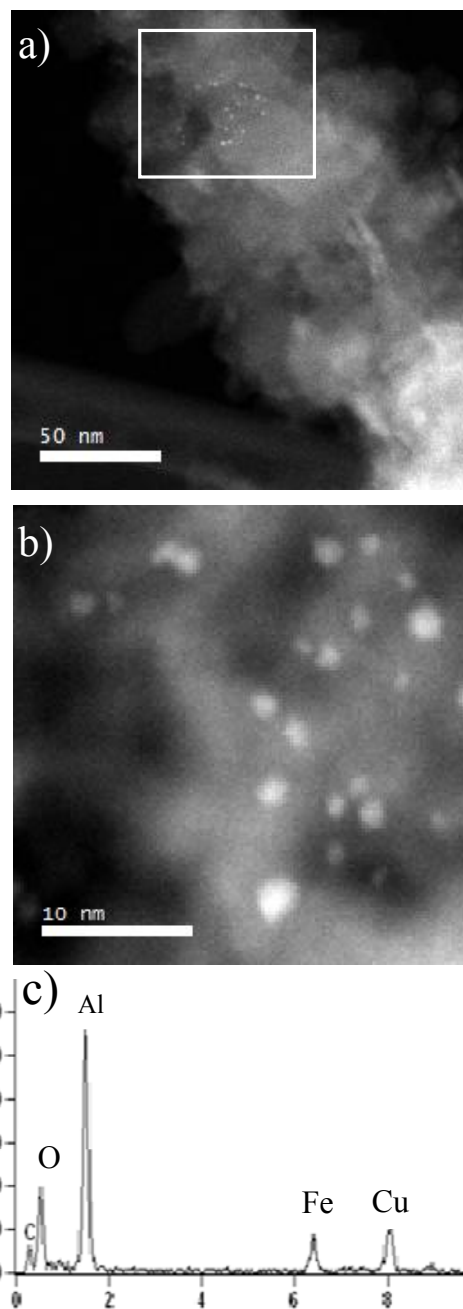


Fig. 3. Typical low (a) and high (b) magnification HAADF-STEM images of the sample milled by 6 h showing small metallic particles (β) inside bayerite phase (α) and (c) EDS analysis of the sample showing Al, Fe and O.

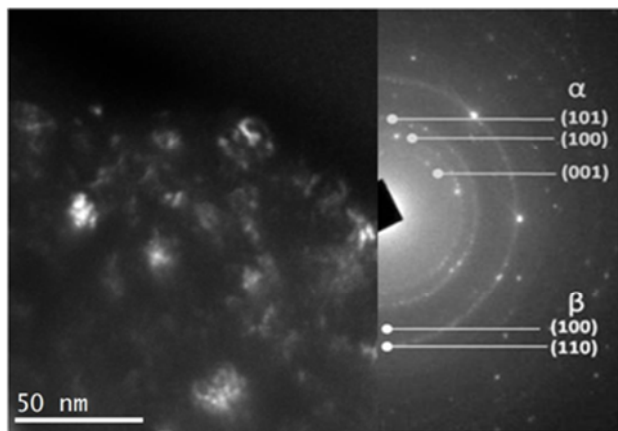


Fig. 4. a) A typical dark-field image of the sample milled for 6 h, showing nanocrystals (b) electron diffraction pattern illustrating the index planes: (101), (100) and (001) corresponding to the α phase as well as planes for β phase: (100), (110).

Figure 5 shows a dark-field TEM image for the sample milled by 1 h, in which small crystallites inside the particles are also observed. The corresponding electron diffraction pattern confirms that these nanocrystals are composed of FeAl intermetallic phase, which is in agreement with X-ray diffraction results. In this sample, reflections belonging to the bayerite phase were not observed.

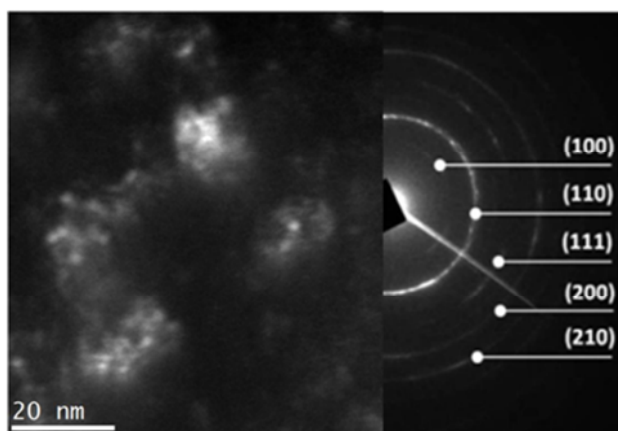


Fig. 5. a) dark-field TEM image of the sample milled for 6 h, b) and c) electron and X-ray diffraction patterns showing the ordered structure of *bcc*-FeAl.

HRTEM studies have been carried out to complement the structural analysis. Figure 6a) exhibits two types of particles which correspond to the coexistence of α -

ceramic and β -metallic phases. HRTEM image (Figure 6b) and its corresponding FFT pattern (Figure 6c) shows d-spacings of 2.9 Å which corresponds to the (100) planes of FeAl phase. Meanwhile, HRTEM image in Figure 6d) and its corresponding FFT pattern (Figure 6e) shows d-spacings of 3.2, 4.3 and 4.7 Å which correspond respectively to (101), (100) and (001) planes of the bayerite structure.

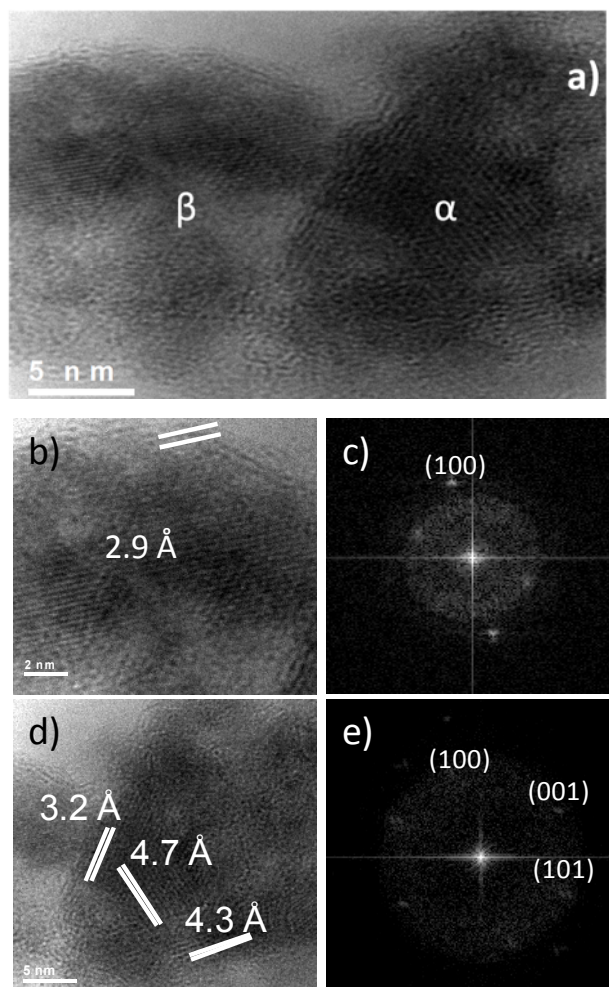


Fig. 6. HRTEM images: a) α -Al(OH)₃ bayerite and β -FeAl intermetallic particles coexisting, b) and c) showing planar spacings which corresponds to the (100) planes of the intermetallic phase (β) respectively, d) and e) showing reflections belonging to the intermetallic phase.

The intermetallic composition Fe₄₀Al₆₀, has aluminum in bcc unit cells which reacts more spontaneously with water to reduce the particle size than pure aluminum with fcc structure. On the other hand, as the reaction proceeds,

a higher quantity of the ceramic phase is formed. Finally, the volumetric relationship of the ceramic phase is evidently larger than the intermetallic phase, so the ceramic phase surrounds the intermetallic phase preventing the diffusion of the humidity toward the metallic particles slowing the rate of HEE.

CONCLUSIONS

In this investigation, the wet-ball milling was successfully used to increase the rate of the HEE of FeAl intermetallic; which reduces the particle size to a nanometer range. Aluminum of the intermetallic alloy reacts with water inside the vial and produces bayerite and hydrogen. The latter being an element that promotes cleavage fracture. As the milling time increased the ceramic phase formed is increased too. The intermetallic phase appears surrounded by the ceramic phase, which is volumetrically greater.

ACKNOWLEDGEMENT

E. Garcia de León want to thank to the Universidad Nacional Autónoma de México, the Universidad Michoacana de San Nicolás de Hidalgo and for the financial support to the National Council for Science and Technology of Mexico (CONACYT) (PhD Scholarship). G. Rosas would like to thank to CONACYT for financial support (48716-25535).

REFERENCES

[1] McKamey C.G., Devan, J. H., Tortorelli, P. F., Sikka, V.K. (1991) "A review of recent developments in Fe₃Al-based alloys" *J. Mater. Res.* 6:1779-1805.

[2] Cahn, R.W. (1996) "Historical Perspective on the Development of Aluminides." *Proceedings of the International Symposium on Nickel and Iron Aluminides ASM*, Materials Park, OH, 3–20.

[3] Testani C., Di Gianfrancesco A., Tassa O., Pocci D. (1996) "FeAl intermetallics and applications: an overview." *Proceedings of the International*

Symposium on Nickel and Iron Aluminides ASM, Materials Park, OH, 213–222.

- [4] Deevi, S.C.V.K. Sikka (1996) "Nickel and iron aluminides: an overview on properties, processing, and applications". *Intermetallics* 4:357-375.
- [5] Esparza R., Rosas G., Ascencio J.A., Pérez R. (2005) "Effects of Minor Element Additions to the Nanocrystalline FeAl Intermetallic Alloy Obtained by Mechanical Alloying", *Mater Manuf Process*, 20(5):823–832.
- [6] Chihuaque J, Patiño-Carachure C., Téllez-Vázquez J.O, Torres-Islas A., Rosas G. (2010) "Microstructural Evaluation During Mechanical Alloying and Air Consolidation of Fe₃Al + (Li, Ni and C) Intermetallic" *Acta Microscopica* 19(3): 305 – 311.
- [7] Salazar M., Albiter A., Rosas G., Pérez R. (2003) "Structural and mechanical properties of the AlFe intermetallic alloy with Li, Ce and Ni additions", *Mater Sci. Eng. A.* 351:154-159.
- [8] Liu C. T., Fu C. L. (1998) "Environmental Embrittlement in FeAl Aluminides" *ISIJ Int.* 31: 1192-1200.
- [9] Chen G. L. Liu C.T. (2001) "Moisture induced environmental embrittlement of intermetallics". *Int. Mater. Rev.* 46: 253 – 270.
- [10] M. Salazar, Rosas G., Perez R. (2005) "Environmental Embrittlement Characteristics of the AlFe and AlFeCu Intermetallic Systems" *J. New Mat. Electrochem. Syst.* 8: 97 - 100.
- [11] C. Patiño-Carachure, E. Garcia-De León, C. Angeles-Chávez, R. Esparza, G. Rosas-Trejo (2009) "Hydrogen embrittlement assisted by ball-milling to obtain AlCuFe nanoparticles". *J. Non- Cryst. Solids.* 355: 1713 – 1718.
- [12] Kravchenko O.V., Semenenko K.N., Bulychev B.M, Kalmykov K.B. (2005) Activation of aluminum metal and its reaction with water", *J. Alloys Compd.* 397:58 - 62.

- [13] Soler L., Candela A.M., Macanas J., Muñoz M., Casado J. (2010)”, Hydrogen generation from water and aluminum promoted by sodium stannate” *Int. J. Hydrogen Energy*. 35: 1038-1048.
- [14] Soler L., Candela A.M., Macanas J., Muñoz M., Casado J. (2009) “In situ generation of hydrogen from water by aluminium corrosion in solutions of sodium aluminate” *J. Power Sources*. 192: 21-26.
- [15] Suryanarayana C. (2001) “Mechanicall alloying” *Prog. Mater. Sci.* 46: 1-184.